NASA/TM—2001-210957/REV1

Simulation of Aircraft Engine Blade-Out Structural Dynamics

Charles Lawrence and Kelly Carney
Glenn Research Center, Cleveland, Ohio

Vicente Gallardo
Ohio Aerospace Institute, Brook Park, Ohio

September 2001

The NASA STI Program Office . . . in Profile

Since its founding, NASA has been dedicated to the advancement of aeronautics and space science. The NASA Scientific and Technical Information (STI) Program Office plays a key part in helping NASA maintain this important role.

The NASA STI Program Office is operated by Langley Research Center, the Lead Center for NASA's scientific and technical information. The NASA STI Program Office provides access to the NASA STI Database, the largest collection of aeronautical and space science STI in the world. The Program Office is also NASA's institutional mechanism for disseminating the results of its research and development activities. These results are published by NASA in the NASA STI Report Series, which includes the following report types:

- TECHNICAL PUBLICATION. Reports of completed research or a major significant phase of research that present the results of NASA programs and include extensive data or theoretical analysis. Includes compilations of significant scientific and technical data and information deemed to be of continuing reference value. NASA's counterpart of peer-reviewed formal professional papers but has less stringent limitations on manuscript length and extent of graphic presentations.

- TECHNICAL MEMORANDUM. Scientific and technical findings that are preliminary or of specialized interest, e.g., quick release reports, working papers, and bibliographies that contain minimal annotation. Does not contain extensive analysis.

- CONTRACTOR REPORT. Scientific and technical findings by NASA-sponsored contractors and grantees.

- CONFERENCE PUBLICATION. Collected papers from scientific and technical conferences, symposia, seminars, or other meetings sponsored or cosponsored by NASA.

- SPECIAL PUBLICATION. Scientific, technical, or historical information from NASA programs, projects, and missions, often concerned with subjects having substantial public interest.

- TECHNICAL TRANSLATION. English-language translations of foreign scientific and technical material pertinent to NASA's mission.

Specialized services that complement the STI Program Office's diverse offerings include creating custom thesauri, building customized data bases, organizing and publishing research results . . . even providing videos.

For more information about the NASA STI Program Office, see the following:

- Access the NASA STI Program Home Page at ***http://www.sti.nasa.gov***

- E-mail your question via the Internet to help@sti.nasa.gov

- Fax your question to the NASA Access Help Desk at 301–621–0134

- Telephone the NASA Access Help Desk at 301–621–0390

- Write to:
  NASA Access Help Desk
  NASA Center for AeroSpace Information
  7121 Standard Drive
  Hanover, MD 21076

NASA/TM—2001-210957/REV1

Simulation of Aircraft Engine Blade-Out Structural Dynamics

Charles Lawrence and Kelly Carney
Glenn Research Center, Cleveland, Ohio

Vicente Gallardo
Ohio Aerospace Institute, Brook Park, Ohio

Prepared for the
Worldwide Aerospace Conference and Technology Showcase
sponsored by MSC Software
Toulouse, France, September 24–26, 2001

National Aeronautics and
Space Administration

Glenn Research Center

September 2001

Available from

NASA Center for Aerospace Information
7121 Standard Drive
Hanover, MD 21076

National Technical Information Service
5285 Port Royal Road
Springfield, VA 22100

Available electronically at http://gltrs.grc.nasa.gov/GLTRS

Document Change History

This printing, numbered as **NASA/TM—2001-210957/REV1, September 2001,** replaces the previous version, **NASA/TM—2001-210957, June 2001**. It contains the following changes:

Page 4: Equation 3 was modified

$$\begin{bmatrix} I_\alpha & 0 \\ 0 & I_\theta \end{bmatrix}\begin{Bmatrix} \ddot{\alpha} \\ \ddot{\theta} \end{Bmatrix} + \left\{\begin{bmatrix} 0 & -2I_\alpha\dot{\bar{\psi}} \\ 2I_\theta\dot{\bar{\psi}} & 0 \end{bmatrix} + \begin{bmatrix} C_{\alpha\alpha} & C_{\alpha\theta} \\ C_{\theta\alpha} & C_{\theta\theta} \end{bmatrix}\right\}\begin{Bmatrix} \dot{\alpha} \\ \dot{\theta} \end{Bmatrix} + \left\{\begin{bmatrix} 0 & -I_\varepsilon\ddot{\bar{\psi}} \\ I_\varepsilon\ddot{\bar{\psi}} & 0 \end{bmatrix} + \begin{bmatrix} K_{\alpha\alpha} & K_{\alpha\theta} \\ K_{\theta\alpha} & K_{\theta\theta} \end{bmatrix}\right\}\begin{Bmatrix} \alpha \\ \theta \end{Bmatrix} = \begin{Bmatrix} F_\alpha \\ F_\theta \end{Bmatrix} \tag{3}$$

Page 4, paragraph 1: The following sentence was added after the first sentence:

($I_\varepsilon = 2I_\alpha = 2I_\theta$ for a symmetric disk.)

Page 5: Equation 5 was modified

$$\begin{bmatrix} \frac{I_p+\varepsilon^2 m}{2} + \frac{\varepsilon^2 m}{2}\cos 2\bar{\psi} & 0 \\ 0 & \frac{I_p+\varepsilon^2 m}{2} - \frac{\varepsilon^2 m}{2}\cos 2\bar{\psi} \end{bmatrix}\begin{Bmatrix} \ddot{\alpha} \\ \ddot{\theta} \end{Bmatrix} + \left\{\begin{bmatrix} 0 & -2\left(\frac{I_p+\varepsilon^2 m}{2} + \frac{\varepsilon^2 m}{2}\cos 2\bar{\psi}\right)\dot{\bar{\psi}} \\ 2\left(\frac{I_p+\varepsilon^2 m}{2} + \frac{\varepsilon^2 m}{2}\cos 2\bar{\psi}\right)\dot{\bar{\psi}} & 0 \end{bmatrix} + \begin{bmatrix} C_{\alpha\alpha} & C_{\alpha\theta} \\ C_{\theta\alpha} & C_{\theta\theta} \end{bmatrix}\right\}\begin{Bmatrix} \dot{\alpha} \\ \dot{\theta} \end{Bmatrix} + \left\{\begin{bmatrix} 0 & -I_\varepsilon\ddot{\bar{\psi}} \\ I_\varepsilon\ddot{\bar{\psi}} & 0 \end{bmatrix} + \begin{bmatrix} K_{\alpha\alpha} & K_{\alpha\theta} \\ K_{\theta\alpha} & K_{\theta\theta} \end{bmatrix}\right\}\begin{Bmatrix} \alpha \\ \theta \end{Bmatrix} = \begin{Bmatrix} F_\alpha \\ F_\theta \end{Bmatrix} \tag{5}$$

Simulation of Aircraft Engine Blade-Out Structural Dynamics

Charles Lawrence and Kelly Carney
National Aeronautics and Space Administration
Glenn Research Center
Cleveland, Ohio 44135

Vicente Gallardo
Ohio Aerospace Institute
Brook Park, Ohio 44142

I. Introduction

The current environment for designing aircraft engine and engine-airframe structural systems requires extensive levels of effort to prepare and integrate models, generate analysis results and post process data. Additionally, the accuracy of the simulations is less than desired, leading to less than optimal designs, costly testing and re-designs and most important, uncertainties in factors of safety. One of the primary concerns of aircraft structure designers is the accurate simulation of the blade-out event and the subsequent windmilling of the engine. Reliable simulations of the blade-out event are required to insure structural integrity during flight as well as to guarantee successful blade-out certification testing. Simulation of windmilling which occurs after blade-out is critical to insure that excessive vibration levels, which may damage the aircraft and endanger passengers, are not experienced. In addition to blade-out and windmilling, structural simulation tools are required to determine structural response during normal aircraft operations and loadings resulting from flight maneuvers. The loads generated by these analyses are critical to the design teams for several components of the airplane structures including engine, nacelle, strut, and wing, as well as the aircraft fuselage.

Currently, a collection of simulation tools is used for aircraft structural design. Detailed high fidelity simulation tools are used to capture the structural loads resulting from blade loss, then these loads are used as input into an overall system model that includes complete structural models of both the engines and the airframe. The detailed simulation includes the time dependent trajectory of the lost blade and it's interactions with the containment structure while the system simulation includes the lost blade loadings and the interactions between the rotating turbomachinery and the remaining aircraft structural components. General-purpose finite element structural analysis codes are typically used and special provisions are made to include transient effects from the blade loss and rotational effects resulting from the engine's turbomachinery. Figures 1 and 2 depict a typical engine structural model and a detailed blade-fan case interaction model, respectively.

A unique characteristic of the blade out event is that the rotational speed of the turbomachinery does not remain constant during the duration of the event. Instead, there is a rapid deceleration where the rotor speed drops suddenly from the normal flight operating rotational speed down to the windmilling speed. (The speed at which the engine is shut down and not producing thrust but is freely rotating as a result of the forward motion of the aircraft.) In severe cases the rotor may be damaged such that the rotor speed drops even lower or more rapidly. Non-constant rotational speed provides a complication to the simulation because in addition to the classical gyroscopic effects that arise from constant rotation speed additional terms must be added to account for the non-constant component of the rotor speed.

In addition to non-constant rotor speed, the blade out event may cause a large enough mass unbalance to significantly alter the inertia properties of the rotor. For normal rotordynamic analysis symmetric inertia properties are assumed. However, the resulting inertia properties after a blade loss will not be symmetric since the blade loss normally is localized at a particular rotor disk segment. Additional treatment in the equations of motion is required to accommodate these effects. The purpose of this paper is to provide a derivation of the non-constant rotor speed and non-symmetric inertia terms and to assess their effects for a sample rotor using a finite element simulation.

II. The Derivation of the Equations of Motion of a Rotating Disk or Rotor Segment

Figure 3 shows the rotor disk or rotor segment used for the present formulation. The primary interest in this paper is the transverse translational and rotational motions of the rotor. To account for these motions, translational and rotational degrees of freedom are established in the x, y and θ, α directions, respectively. Small lateral and angular deflections are assumed except for the spin and rotor speed about the disk centerline, which is allowed to be large. The axial displacement and spin is not included as degrees of freedom but as described in the formulation, their effects are included in the transverse motions. Once the equations of motion are determined for an individual rotor disk or segment they are assembled to form a complete rotor model using conventional finite element assembly techniques.

Since most analysts use finite element analysis tools for engine and engine-airframe analysis it is desirable to provide a rotordynamic formulation that can be directly implemented into existing finite element analysis codes. To meet this criterion the equations of motion are derived in fixed (inertial) coordinates since most finite element codes utilize fixed coordinates. The present formulation also assumes that the rotor model can be adequately represented with a beam type model. This restriction requires that all the finite element nodes be placed on the spin axis and that any off axis inertial properties be transformed to the rotor centerline.

The equations of motion in the translational degrees of freedom x, y can be derived in the standard Newtonian way, or by the Lagrangian operation in the kinetic energy. For these degrees of freedom, DOF's, the equations of motion are:

$$\begin{bmatrix} M & 0 \\ 0 & M \end{bmatrix}\begin{Bmatrix} \ddot{x} \\ \ddot{y} \end{Bmatrix}+\begin{bmatrix} C_{xx} & C_{xy} \\ C_{yx} & C_{yy} \end{bmatrix}\begin{Bmatrix} \dot{x} \\ \dot{y} \end{Bmatrix}+\begin{bmatrix} K_{xx} & K_{xy} \\ K_{yx} & K_{yy} \end{bmatrix}\begin{Bmatrix} x \\ y \end{Bmatrix}=\begin{Bmatrix} F_x \\ F_y \end{Bmatrix} \tag{1}$$

Where M, C, and K are the rotor segment's mass, damping and stiffness, respectively and F_x and F_y are external forces. Note there is no inertial coupling with the pitch and yaw rotational degrees of freedom. (There will be coupling between these DOF's from the rotor's elastic properties and possibly from damping, tip rub or other mechanisms.) There also are no rotational effects appearing in this equation.

In the case of a highly unbalanced or non-axisymmetric bladed disk, the equations of motion must be modified to account for the mass eccentricity. For this situation, the equation of motion is:

$$\begin{bmatrix} M & 0 \\ 0 & M \end{bmatrix}\begin{Bmatrix} \ddot{x} \\ \ddot{y} \end{Bmatrix}+\begin{bmatrix} C_{xx} & C_{xy} \\ C_{yx} & C_{yy} \end{bmatrix}\begin{Bmatrix} \dot{x} \\ \dot{y} \end{Bmatrix}+\begin{bmatrix} K_{xx} & K_{xy} \\ K_{yx} & K_{yy} \end{bmatrix}\begin{Bmatrix} x \\ y \end{Bmatrix}= \begin{Bmatrix} F_x \\ F_y \end{Bmatrix}+\begin{Bmatrix} \varepsilon m\ddot{\overline{\psi}}\sin\overline{\psi} \\ -\varepsilon m\ddot{\overline{\psi}}\cos\overline{\psi} \end{Bmatrix}+\begin{Bmatrix} \varepsilon m\dot{\overline{\psi}}^2\cos\overline{\psi} \\ \varepsilon m\dot{\overline{\psi}}^2\sin\overline{\psi} \end{Bmatrix} \tag{2}$$

Where εm is the mass eccentricity and $\dot{\overline{\psi}}$ is the specified rotor speed. The second and third terms on the right hand side represent the forces from the rate of change in the rotor speed and the centrifugal force, respectively. It is interesting to note that with a mass eccentricity the rotational term, $\overline{\psi}$, appears in the translational equation of motion (last two terms on r.h.s of (2)) whereas without eccentricity there are no rotational effects in equation (2). It is also important to note that for non-constant rotor speeds the rotor speed must be integrated over time to determine $\overline{\psi}$.

The equations of motion in the rotational degrees of freedom are derived somewhat differently since the inclusion of spin effects complicates the derivation. For these equations it is most convenient to use Euler angles then transform the resulting equations to ground fixed finite element coordinates. Davis (Ref. 1) has previously reported this approach. Davis' equations contain nonlinearities of the 3rd or 4th order, which may be neglected for practical engineering applications. Although the elastic and damping forces may exhibit nonlinear behavior in gas turbine engines, the rotor kinetic terms are normally linear. Using the Davis results verbatim and neglecting higher order terms the rotational equation of motion for an axisymmetric rotor segment (without unbalance) is:

$$\begin{bmatrix} I_\alpha & 0 \\ 0 & I_\theta \end{bmatrix}\begin{Bmatrix} \ddot{\alpha} \\ \ddot{\theta} \end{Bmatrix}+\left\{\begin{bmatrix} 0 & -2I_\alpha\dot{\bar{\psi}} \\ 2I_\theta\dot{\bar{\psi}} & 0 \end{bmatrix}+\begin{bmatrix} C_{\alpha\alpha} & C_{\alpha\theta} \\ C_{\theta\alpha} & C_{\theta\theta} \end{bmatrix}\right\}\begin{Bmatrix} \dot{\alpha} \\ \dot{\theta} \end{Bmatrix}+ \left\{\begin{bmatrix} 0 & -I_\varepsilon\ddot{\bar{\psi}} \\ I_\varepsilon\ddot{\bar{\psi}} & 0 \end{bmatrix}+\begin{bmatrix} K_{\alpha\alpha} & K_{\alpha\theta} \\ K_{\theta\alpha} & K_{\theta\theta} \end{bmatrix}\right\}\begin{Bmatrix} \alpha \\ \theta \end{Bmatrix}=\begin{Bmatrix} F_\alpha \\ F_\theta \end{Bmatrix} \tag{3}$$

Where I_ε is the mass moment of inertia about the spin axis of the balanced disk, and I_α and I_θ are the moments of inertia about the α and θ axis, respectively. ($I_\varepsilon = 2I_\alpha = 2I_\theta$ for a symmetric disk.) The $I_\varepsilon\dot{\bar{\psi}}$ terms correspond to the well-known gyroscopic terms while the $I_\varepsilon\ddot{\bar{\psi}}$ terms correspond to the spooldown rate. The later term is skew-symmetric and proportional to the displacements. This term appears similar in form to internal rotor damping that has been shown to have a destabilizing effect on rotordynamic response (Ref. 3).

Similar to the translational equations of motion, in the case of a highly unbalanced or non-axisymmetric bladed disk, the inertia properties must also be corrected. An unbalanced or non-symmetric bladed disk has two unequal transverse mass moments of inertia about orthogonal principal axes. By considering the bladed disk non-axisymmetry, as arising from an eccentricity, ε, such as from blade loss, the pitch and yaw inertia is defined as (See Chapter 7 of Ref. 4):

$$I_\alpha = \frac{I_p + \varepsilon^2 m}{2} + \frac{\varepsilon^2 m}{2}\cos 2\bar{\psi} \tag{4a}$$

$$I_\theta = \frac{I_p + \varepsilon^2 m}{2} - \frac{\varepsilon^2 m}{2}\cos 2\bar{\psi} \tag{4b}$$

$$I_\varepsilon = I_p + \varepsilon^2 m \tag{4c}$$

Where I_p is the mass moment of inertia about the spin axis with the unbalance mass removed. When the disk is rotating, the transverse mass moments of inertia about the ground based pitch and yaw axes (α and θ) vary twice per revolution. This follows from the definition of the transverse mass moments of inertia in the ground fixed reference frame. For subsequent discussion in this paper the terms containing $\varepsilon^2 m$ will be referred to as the "parametric terms" since they correspond to the parametric excitation from the mass unbalance.

Replacing the inertia terms in equation 3 with the inertia's in equation 4 yields:

$$\begin{bmatrix} \frac{I_p+\varepsilon^2 m}{2}+\frac{\varepsilon^2 m}{2}\cos\ 2\overline{\psi} & 0 \\ 0 & \frac{I_p+\varepsilon^2 m}{2}-\frac{\varepsilon^2 m}{2}\cos\ 2\overline{\psi} \end{bmatrix} \begin{Bmatrix} \ddot{\alpha} \\ \ddot{\theta} \end{Bmatrix}$$

$$+\left\{ \begin{bmatrix} 0 & -2\left(\frac{I_p+\varepsilon^2 m}{2}+\frac{\varepsilon^2 m}{2}\cos\ 2\overline{\psi}\right)\dot{\overline{\psi}} \\ 2\left(\frac{I_p+\varepsilon^2 m}{2}+\frac{\varepsilon^2 m}{2}\cos\ 2\overline{\psi}\right)\dot{\overline{\psi}} & 0 \end{bmatrix} + \begin{bmatrix} C_{\alpha\alpha} & C_{\alpha\theta} \\ C_{\theta\alpha} & C_{\theta\theta} \end{bmatrix} \right\} \begin{Bmatrix} \dot{\alpha} \\ \dot{\theta} \end{Bmatrix} \quad (5)$$

$$+\left\{ \begin{bmatrix} 0 & -I_\varepsilon\ddot{\overline{\psi}} \\ I_\varepsilon\ddot{\overline{\psi}} & 0 \end{bmatrix} + \begin{bmatrix} K_{\alpha\alpha} & K_{\alpha\theta} \\ K_{\theta\alpha} & K_{\theta\theta} \end{bmatrix} \right\} \begin{Bmatrix} \alpha \\ \theta \end{Bmatrix} = \begin{Bmatrix} F_\alpha \\ F_\theta \end{Bmatrix}$$

III. Results

The above equations were programmed into a finite element code to perform simulations and assess the effects of the various terms in the equations of motion. Figure 4 shows the finite element model used for the subsequent simulations. The model consists of 5 beam elements, 6 nodes and 36 degrees of freedom. Relatively rigid springs attach node 6 to ground in both the translational and rotational directions. Although axial and torsional degrees of freedom are included in the finite element model they are not used in the present study. All of the rotational inertia (I_p, I_α, I_θ) is concentrated in the disk at the rotor tip. A 5% structural damping at 60 Hz was used. The present model is the same as the model used by Boeing in Sample Problem One of their documentation for rotordynamic analysis (Ref. 2). A good match was found when comparing the present model with the Campbell diagram in the Boeing documentation.

Figure 5 shows the rotor spool down speed profile used for the transient simulations. This speed profile is representative of the profile that a rotor may undergo as a result of a blade loss event. The actual spooldown profile is continuous but is often approximated by a series of discontinuous straight lines as shown in the figure. Up until time = 0.0, the rotor is spinning at a constant rate, then at time = 0.0, a blade is released and the rotor begins to shut down. Two different speed profiles were used for the simulations: a slower one where it takes 1.0 second for the rotor to come to rest and a second profile where the rotor comes to rest in 0.10 second. Both profiles were used to study the effect that spooldown rate has on transient response.

Figures 6a and 6b show transient results for the two spooldown speed profiles. The only loading on the rotor is from a mass unbalance located at the rotor disk. A total of 263,000 time steps of $4x10^{-6}$ second were used to generate a time history of 1. 0 seconds. The unbalance mass was equal to 100. oz.-inches.

Figure 6a shows the radial tip displacement for three cases; 1) no gyroscopic terms included, 2) gyroscopics included, and 3) all terms including spooldown rate terms included. As shown in the figure, there is considerable difference between including and not including the gyroscopic terms. The peak displacement without gyroscopics terms is near 0.35 inch while with the gyroscopics terms the maximum radial displacement is 0.6 inch. The difference between results that include the spooldown rate terms and those that do not are very minor indicating that the rate terms have little effect for this combination of rotor characteristics and spooldown profile.

Figure 6b shows the rotor radial displacement for a 0.1 second spooldown. For this case the spooldown rate terms are larger since the spooldown is faster and it was expected that there would be a more significant difference between the transient result when neglecting or including these terms. There is a more noticeable difference. The peak displacement without the spooldown rate terms is 0.142 inch while without the terms it is 0.148 inch (4% difference). While the spooldown rate term is more important for faster spooldowns, the total effect of the rotating unbalance becomes smaller since the rotor is spinning for less time. This effect is exhibited by the peak displacement for the 1.0 second spooldown being 0.6 inch while for the 0.1 second spooldown the peak displacement is only 0.148 inch.

The transient results presented in the previous figures were generated by using a relatively small mass unbalance ($\varepsilon^2 m = 0.2\%$ of I_p). A larger mass unbalance was used to examine the effect that the magnitude of the mass unbalance has on the transient response. For the results in figure 7 a mass unbalance, $\varepsilon^2 m$, of .3945 in^2-lbm was used. This unbalance is equal to 5% of the polar inertia, I_p. While the radial tip displacement is larger due to the larger unbalance there is no significant difference between the results when the spooldown rate terms are included. Furthermore, there is no significant difference when the parametric terms are included, either.

Figures 8a and 8b show the translational and rotational forces, respectively, at the rotor disk resulting from the unbalance. The forces were generated for a spooldown speed of 0.10 seconds. As expected, the translational force is dominated by the $\dot{\bar{\Psi}}^2 \varepsilon m$ term in the translational equation of motion. The translational force resulting from the spooldown rate term is much smaller and is 90° out of phase of the $\dot{\bar{\Psi}}^2 \varepsilon m$ term. There is a small discontinuity in both force profiles at 0.02 seconds due to the change in slope of the rotor speed profile. During the early part of the transient, the parametric force is of similar magnitude to the spooldown rate force but is of the opposite sign, thus the two forces tend to counteract each other.

The moments shown in figure 8b also follow the expected trend. The gyroscopic moment is the largest of the moments and the spooldown and parametric moments are much smaller. The moment resulting from the spooldown term is, similarly to the transitional force, 90° out of phase with the gyroscopic force. The moment resulting from the parametric term is at twice the frequency of the other two moments. During half the time the parametric moment contributes to the gyroscopic moment and during the other half it offsets the gyroscopic moment.

Figure 9 shows the radial tip displacement for a 0.10 second spooldown and a mass unbalance, $\varepsilon^2 m$, of .3945 in^2-lbm. With the larger mass unbalance and the faster spooldown speed it was expected that the spooldown rate terms and the parametric terms would have a larger effect on the displacements thus showing a larger difference than when these terms are not included. Although there is some difference in the radial displacements, the displacements are for the most part very similar regardless of whether these terms are included or not. The difference in the peak displacement is about 3% (3.6 inch vs. 3.5 inch).

Figure 10 shows the steady state displacement amplitude at the rotor disk resulting from a constant unbalance load. Three sets of data were computed: without inclusion of the spooldown rate terms, with a spooldown rate of 1.0 second and with a spooldown rate of 0.10 seconds. Generating these curves with a spooldown rate is somewhat fictitious since it is physically impossible to have a spooldown simultaneously with a steady state unbalance excitation. However, it is informative to perform this analysis because it provides insight into the effect of the spooldown terms on the dynamic characteristics of the rotor. As shown in the figure, the slower spooldown (1.0 seconds) had little effect on the response while the faster spooldown rate (0.10 seconds) had more of an effect on the steady state amplitude. It was expected that the spooldown effect would alter the RPM where the peak amplitude occurs but this effect was not observed with the two spooldown rates studied.

Figure 11 shows the effect that the parametric excitation terms have on the steady state displacement amplitude. Performing a transient simulation at a constant rotational speed generated the results presented in this figure. A mass unbalance, $\varepsilon^2 m$, of .3945 in^2-lbm was applied at time 0.0, After a period of time the initial transient resulting from the sudden unbalance dissipated and the displacements reached a steady state amplitude. The steady state displacement was recorded and a new transient analysis was performed at a new rotational speed. As shown in the figure, the parametric term has a very significant effect on the rotor response. Not only is there a change in the peak amplitude but there also is a shift in the location of the critical speed. Without the parametric terms, the peak amplitude is 33 inch and the critical speed is 2950 RPM while with the parametric terms the peak amplitude is 43 inch and the critical speed is 2825 RPM. It was expected that the critical speed would be lower with the parametric terms included since mass is added to the rotor from the rotor unbalance. In a real application the mass unbalance would be subtracted from the rotor and the critical speeds would be higher. These results are very important, because after a blade loss the rotor continues to rotate at a steady windmilling

rotational speed and the disk where the blade loss occurred is in fact unbalanced leading to a parametric excitation. Neglecting this term may lead to very large under predictions of the rotor response. It is particularly important that the mass unbalance be included in the acceleration terms and probably less important that they be included in the velocity and displacement coefficient matrices.

IV. Summary

The present study provides the equations of motion for rotordynamic response including the effect of spooldown speed and rotor unbalance and examines the effects of these terms on a sample cantilevered rotor. The results of this study, although obtained for a simple rotor, may be extrapolated to more complex rotors and complete engine-airframe systems. The effect of spooldown speed is found to be greater with increasing spooldown rate. However, at faster spooldown rates, the duration of the excitation is shorter and the rotor has less time to respond thus generating overall reduced responses in comparison to slower spooldown rates. In fact it was difficult to identify loading combinations with the present sample problem where the spooldown effect had a significant effect. The spooldown rate terms appear in the equations of motion similarly to internal rotor damping but do not induce the same instabilities as internal damping since the spooldown effect is transient and of a short enough duration to not enable instabilities to develop. The parametric term resulting from the mass unbalance has a more significant effect on the rotordynamic response than does the spooldown term. The parametric term affects both the peak amplitudes as well as the resonant frequencies of the rotor. The effect is more pronounced for larger mass unbalances.

V. References

1. Davis, R. R., "Enhanced rotor modeling tailored for rub dynamic stability analysis and simulation", NASA, Lewis Research Center, Rotordynamic Instability Problems in High-Performance Turbomachinery, 1988, p 431-444.

2. http://maestro.lerc.nasa.gov/ea_sim/document/

3. Zorzi, E. S. and Nelson, H. D., "Finite element simulation of rotor-bearing systems with internal damping", ASME PAPER 76-GT-89, 1976

4. Greenwood, D. T., Principles of dynamics, Prentice-Hall, Inc., 1965.

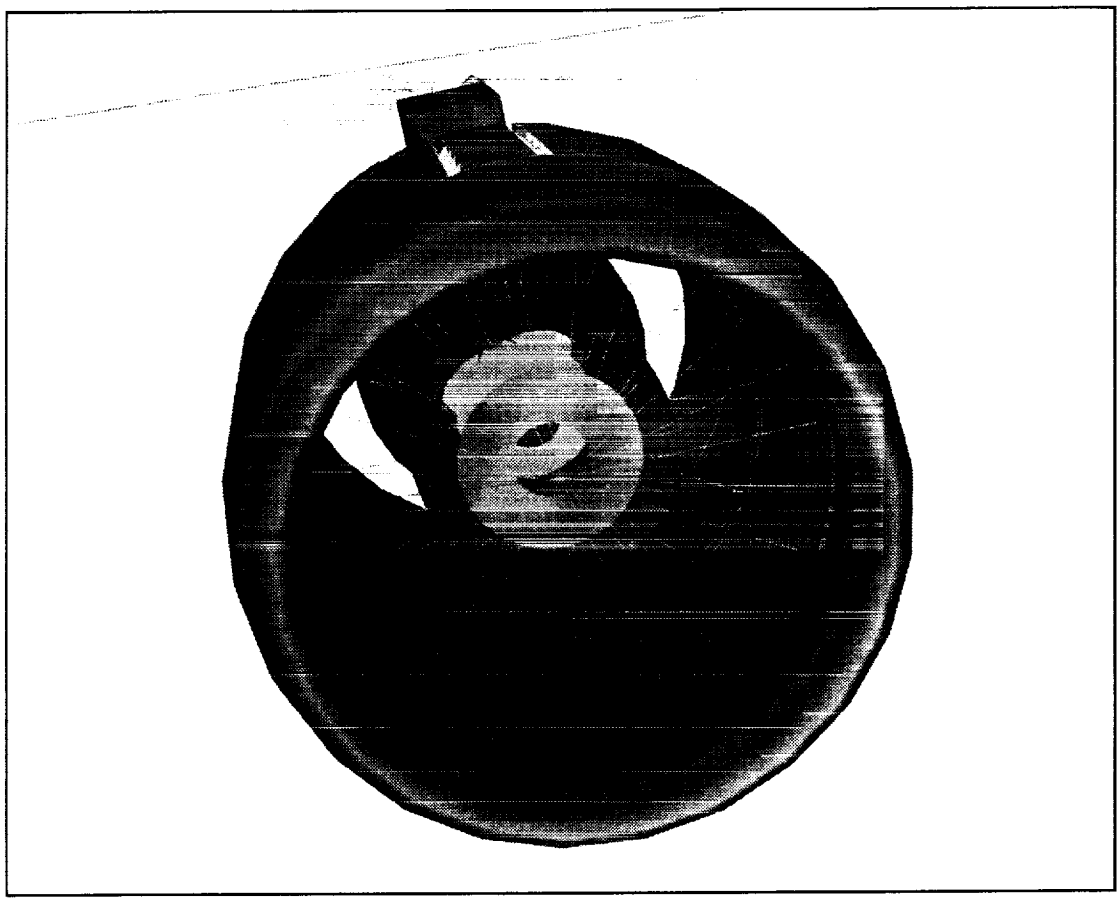

Figure 1: Generic Engine System Model

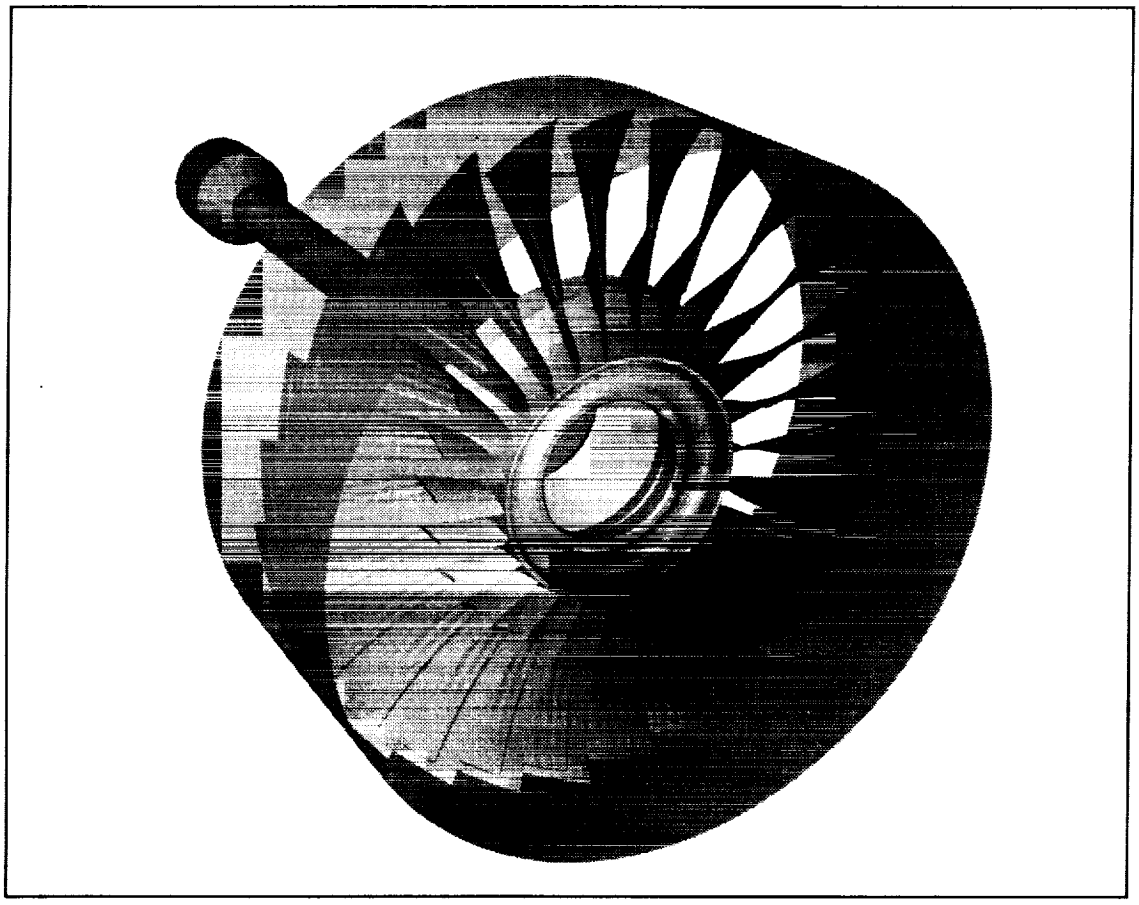

Figure 2: Detailed Blade-Fan Case Interaction Model

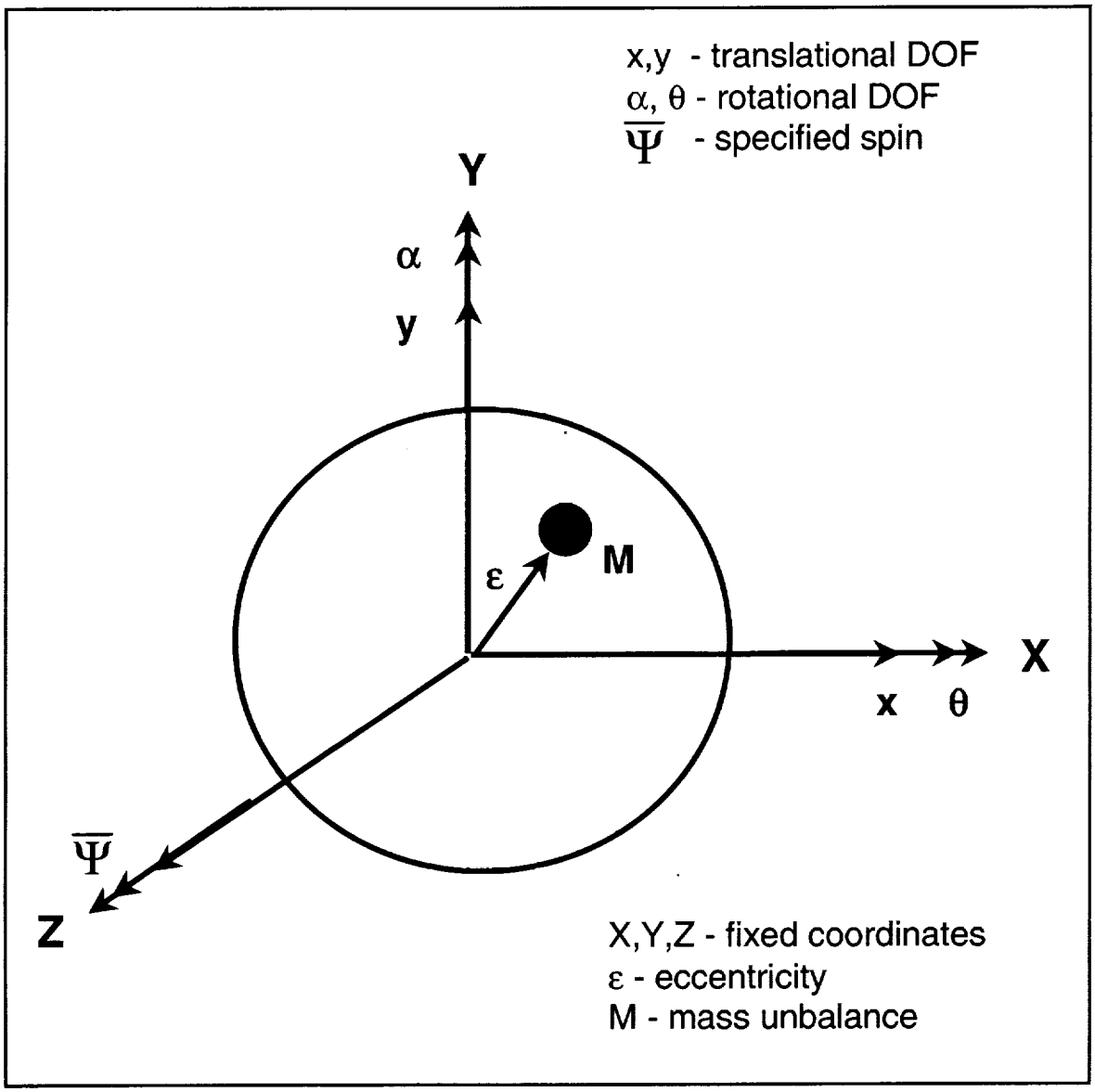

Figure 3: Rotor Segment with Mass Unbalance

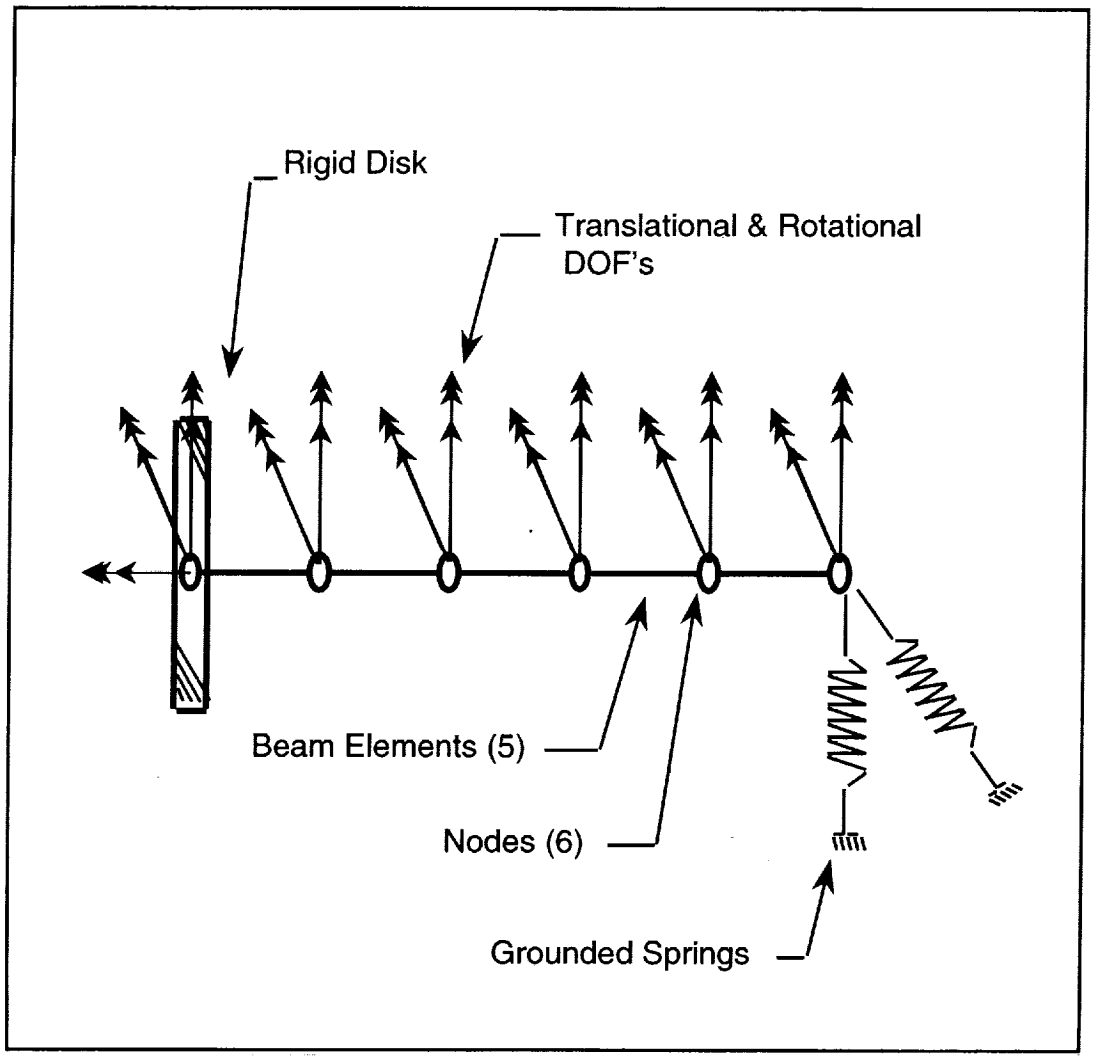

Figure 4: Rotor Finite Element Model

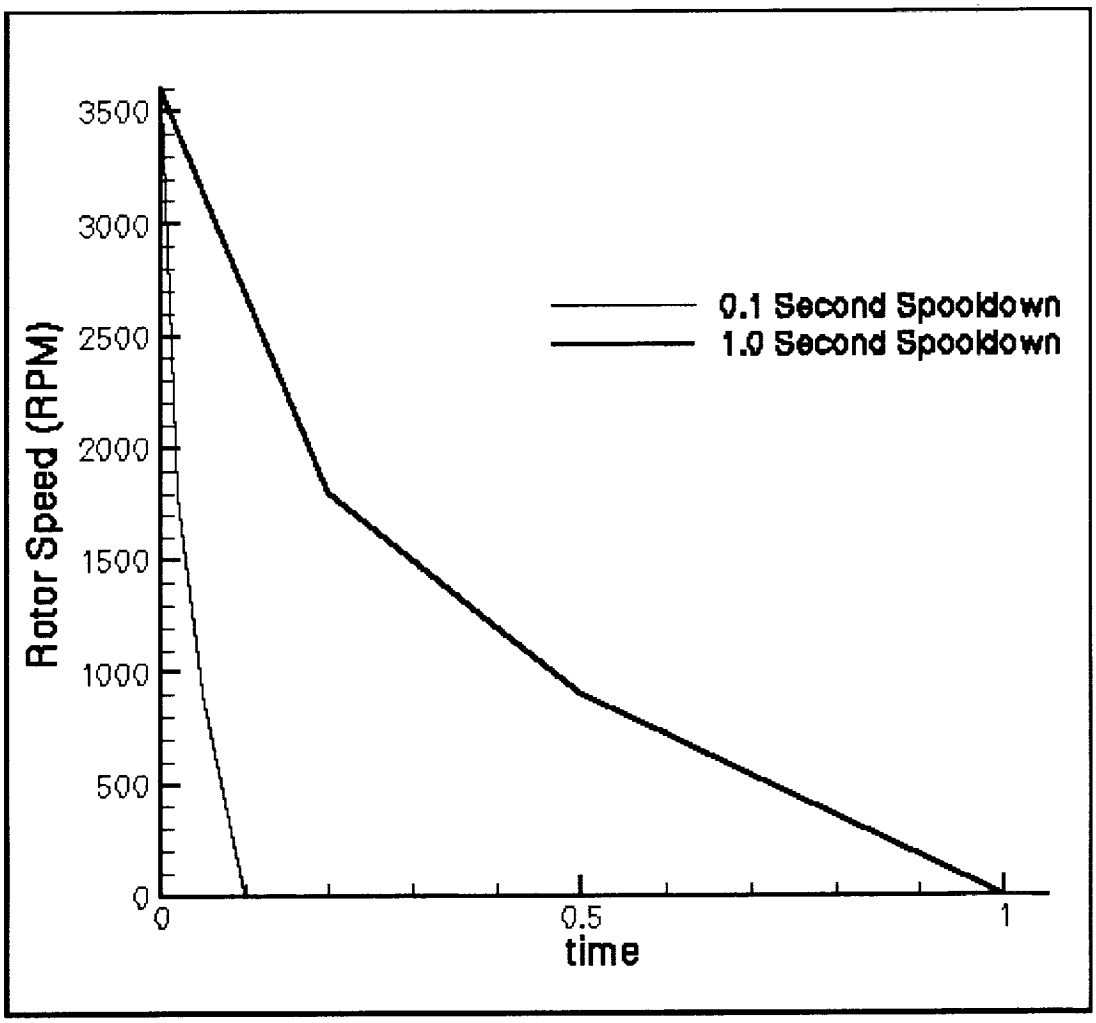

Figure 5: Rotor Spooldown Speed Profile

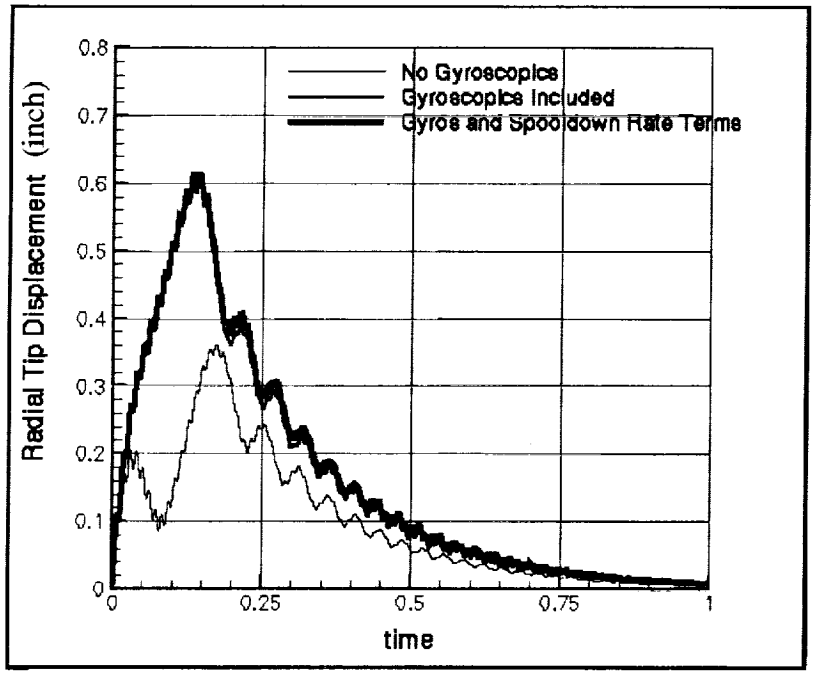

(a) 1.0 Second Spooldown

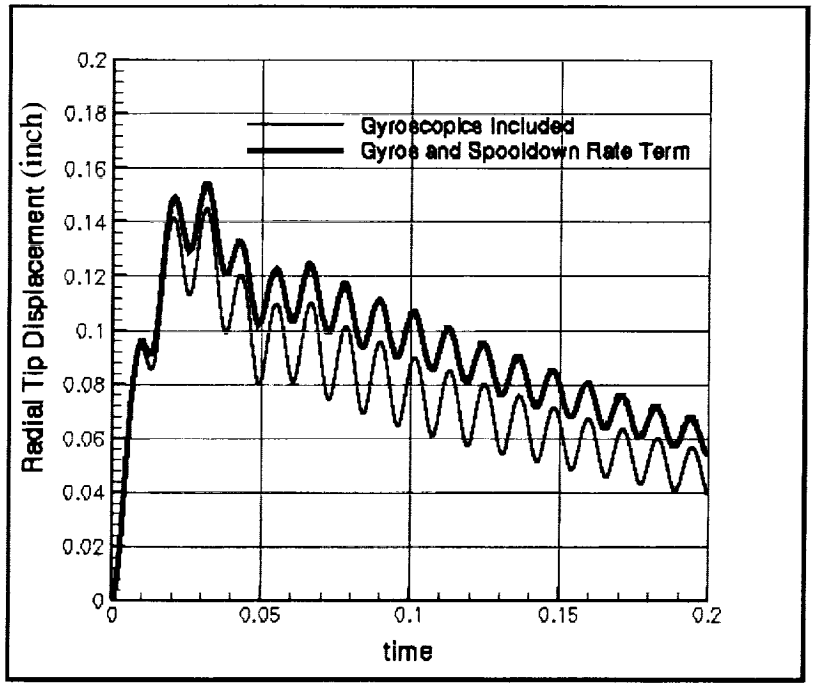

(b) 0.1 Second Spooldown

Figure 6: Rotor Transient Displacement

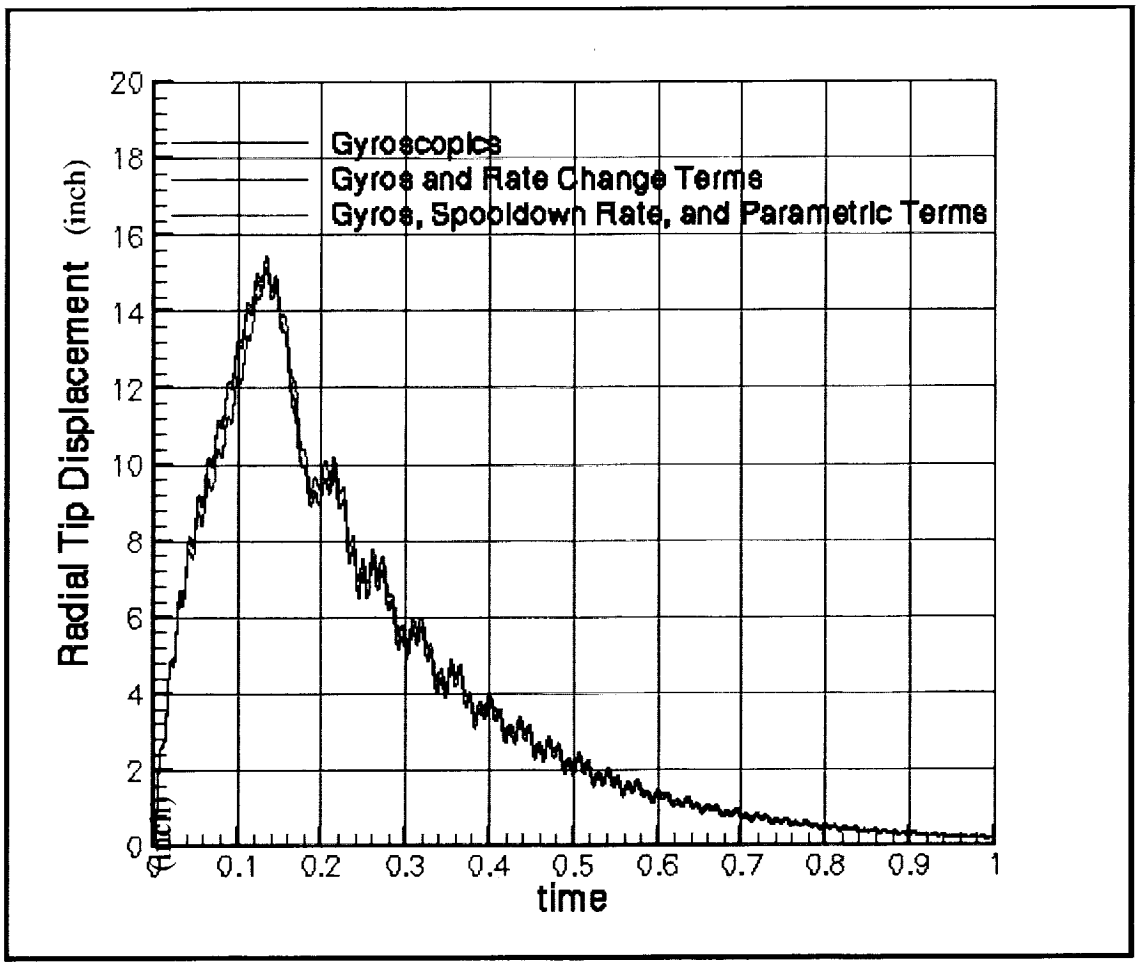

Figure 7: Rotor Transient Displacement
(Spooldown = 1.0 Second, $\varepsilon^2 m$ = .3945 in.^{2}-lbm)

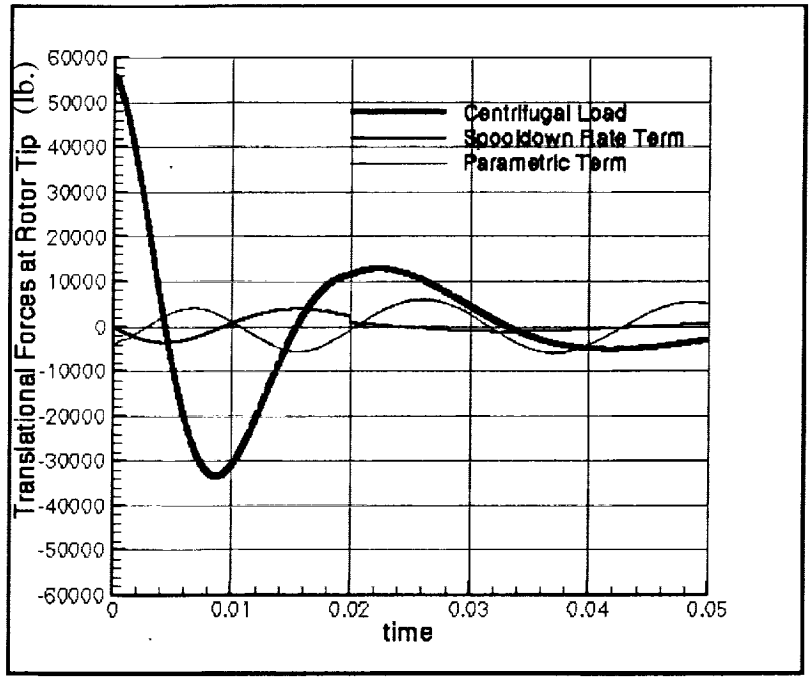

(a) Forces

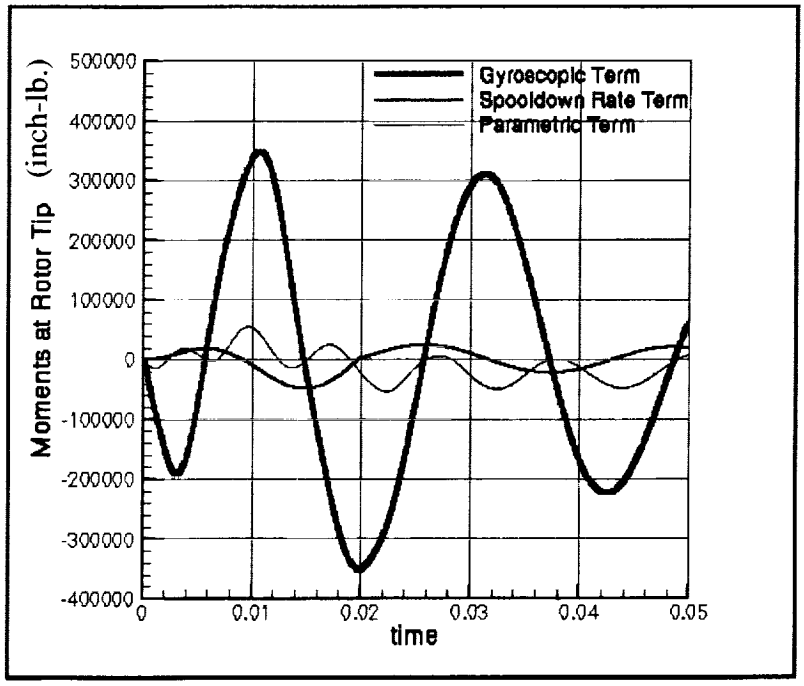

(b) Moments

Figure 8: Rotor Loads at Disk

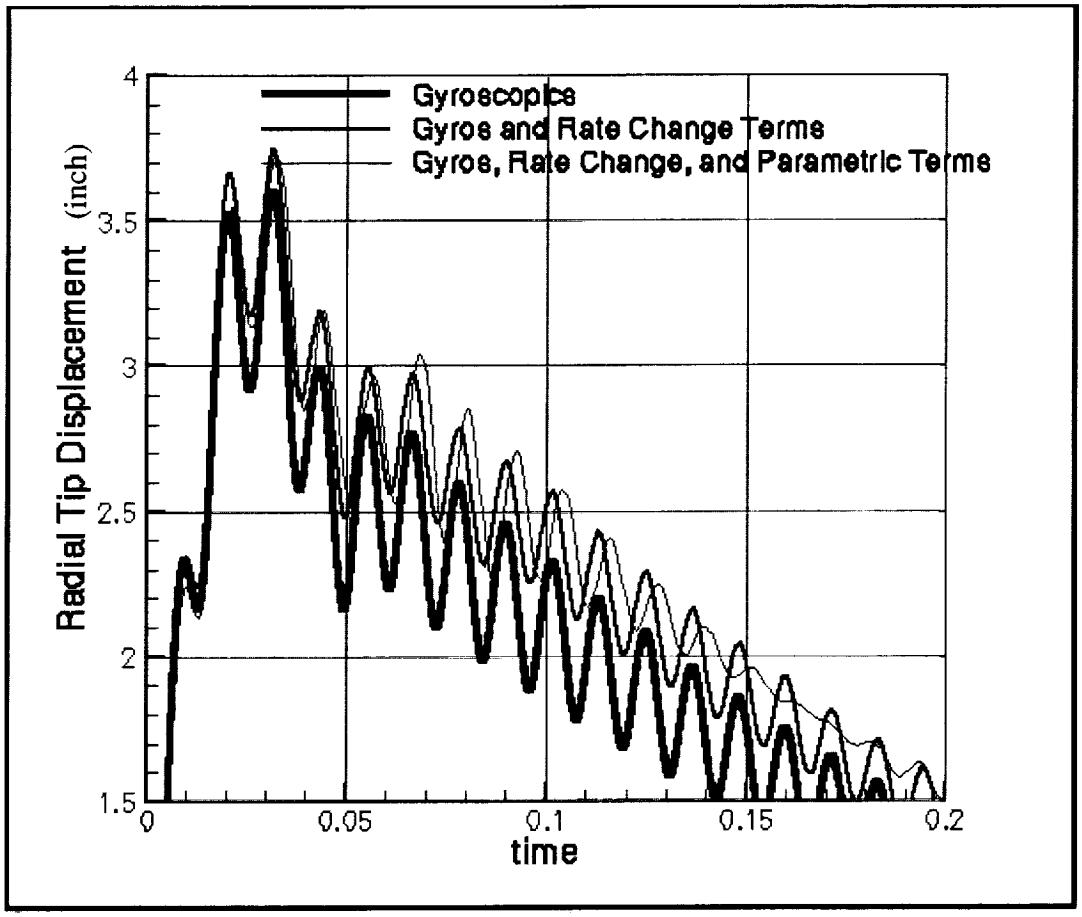

Figure 9: Rotor Displacement for Large Unbalance
and Rapid Spooldown

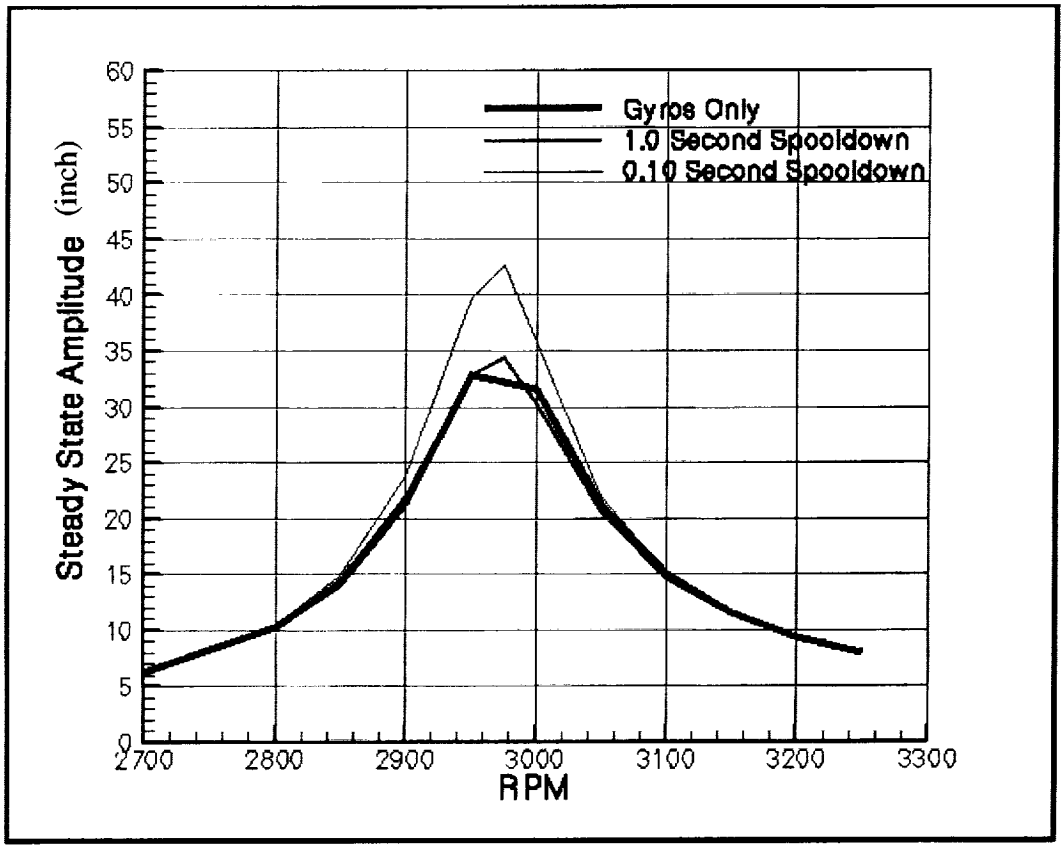

Figure 10: Effect of Spooldown on
Resonant Frequencies

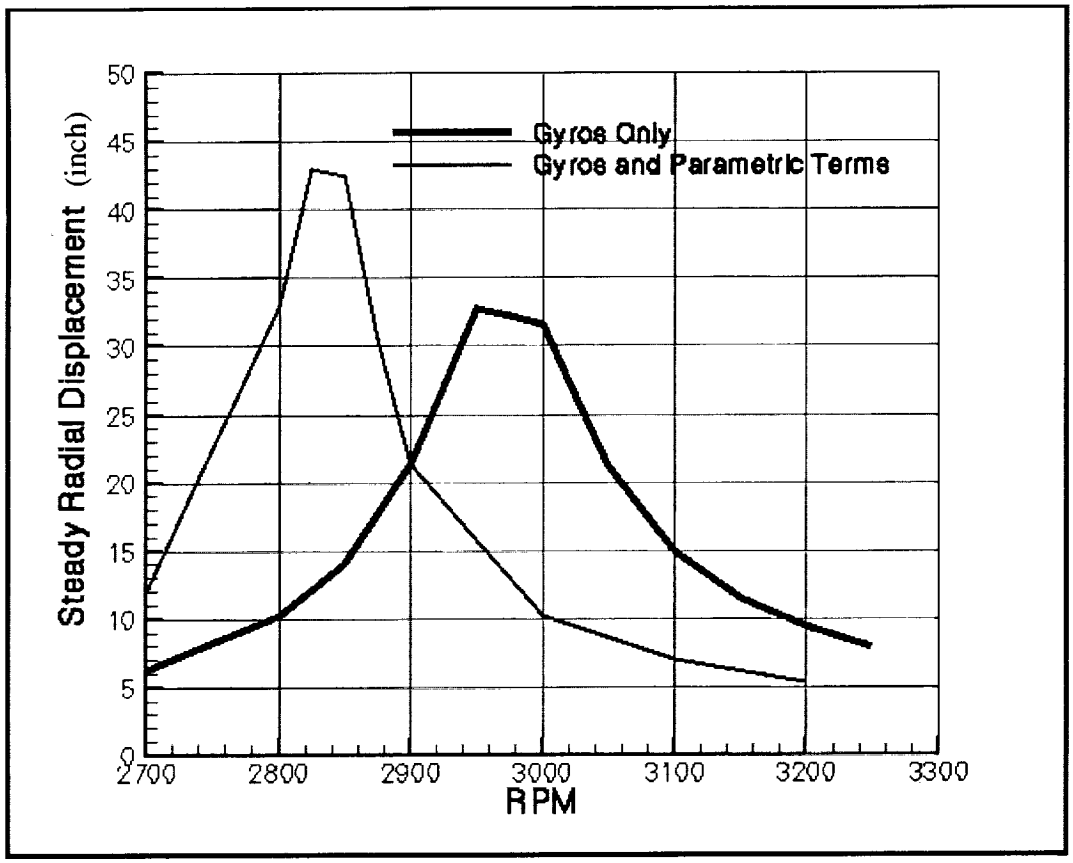

Figure 11: Effect of Parametric Term on
Steady State Amplitude

REPORT DOCUMENTATION PAGE

Form Approved
OMB No. 0704-0188

1. AGENCY USE ONLY (*Leave blank*)	2. REPORT DATE	3. REPORT TYPE AND DATES COVERED
	September 2001	Technical Memorandum

4. TITLE AND SUBTITLE

Simulation of Aircraft Engine Blade-Out Structural Dynamics

5. FUNDING NUMBERS

WU–708–24–13–00

6. AUTHOR(S)

Charles Lawrence, Kelly Carney, and Vicente Gallardo

7. PERFORMING ORGANIZATION NAME(S) AND ADDRESS(ES)

National Aeronautics and Space Administration
John H. Glenn Research Center at Lewis Field
Cleveland, Ohio 44135–3191

8. PERFORMING ORGANIZATION REPORT NUMBER

E–12812-1

9. SPONSORING/MONITORING AGENCY NAME(S) AND ADDRESS(ES)

National Aeronautics and Space Administration
Washington, DC 20546–0001

10. SPONSORING/MONITORING AGENCY REPORT NUMBER

NASA TM—2001-210957-REV1

11. SUPPLEMENTARY NOTES

This printing, numbered as NASA/TM—2001-210957/REV1, September 2001, replaces the previous version, NASA/TM—2001-210957, June 2001. Prepared for the Worldwide Aerospace Conference and Technology Showcase sponsored by MSC Software, Toulouse, France, September 24–26, 2001. Charles Lawrence and Kelly Carney, NASA Glenn Research Center; and Vicente Gallardo, Ohio Aerospace Institute, 22800 Cedar Point Road, Brook Park, Ohio 44142. Responsible person, Charles Lawrence, organization code 5930, 216–433–6048.

12a. DISTRIBUTION/AVAILABILITY STATEMENT

Unclassified - Unlimited
Subject Categories: 39 and 07 Distribution: Nonstandard

Available electronically at http://gltrs.grc.nasa.gov/GLTRS

This publication is available from the NASA Center for AeroSpace Information, 301–621–0390.

12b. DISTRIBUTION CODE

13. ABSTRACT (*Maximum 200 words*)

A primary concern of aircraft structure designers is the accurate simulation of the blade-out event and the subsequent windmilling of the engine. Reliable simulations of the blade-out event are required to insure structural integrity during flight as well as to guarantee successful blade-out certification testing. The system simulation includes the lost blade loadings and the interactions between the rotating turbomachinery and the remaining aircraft structural components. General-purpose finite element structural analysis codes such as MSC NASTRAN are typically used and special provisions are made to include transient effects from the blade loss and rotational effects resulting from the engine's turbomachinery. The present study provides the equations of motion for rotordynamic response including the effect of spooldown speed and rotor unbalance and examines the effects of these terms on a cantilevered rotor. The effect of spooldown speed is found to be greater with increasing spooldown rate. The parametric term resulting from the mass unbalance has a more significant effect on the rotordynamic response than does the spooldown term. The parametric term affects both the peak amplitudes as well as the resonant frequencies of the rotor.

14. SUBJECT TERMS

Turbomachinery; Structural dynamics

15. NUMBER OF PAGES

25

16. PRICE CODE

17. SECURITY CLASSIFICATION OF REPORT	18. SECURITY CLASSIFICATION OF THIS PAGE	19. SECURITY CLASSIFICATION OF ABSTRACT	20. LIMITATION OF ABSTRACT
Unclassified	Unclassified	Unclassified	